



Aalborg Universitet

AALBORG UNIVERSITY
DENMARK

Sea Slot Cone Generator Overtopping Performance in 3D Conditions

Margheritini, Lucia; Vicinanza, Diego; Frigaard, Peter

Published in:

ISOPE - International Offshore and Polar Engineering Conference. Proceedings

Publication date:
2008

Document Version
Publisher's PDF, also known as Version of record

[Link to publication from Aalborg University](#)

Citation for published version (APA):

Margheritini, L., Vicinanza, D., & Frigaard, P. (2008). Sea Slot Cone Generator Overtopping Performance in 3D Conditions. *ISOPE - International Offshore and Polar Engineering Conference. Proceedings*, (18).

General rights

Copyright and moral rights for the publications made accessible in the public portal are retained by the authors and/or other copyright owners and it is a condition of accessing publications that users recognise and abide by the legal requirements associated with these rights.

- Users may download and print one copy of any publication from the public portal for the purpose of private study or research.
- You may not further distribute the material or use it for any profit-making activity or commercial gain
- You may freely distribute the URL identifying the publication in the public portal -

Take down policy

If you believe that this document breaches copyright please contact us at vbn@aub.aau.dk providing details, and we will remove access to the work immediately and investigate your claim.

Sea Slot Cone Generator overtopping performance in 3D conditions

L. Margheritini¹, D. Vicinanza², P. Frigaard¹.

¹Department of Civil Engineering, Aalborg University,
Aalborg, Denmark.

²Centro Interdipartimentale di Ricerca in Ingegneria Ambientale, Seconda Università di Napoli,
Aversa (Caserta), Italy.

ABSTRACT This note describes the influence of wave spreading, directionality and local bathymetry on the efficiency of the Sea Slot Cone Generator (SSG) wave energy converter pilot plant in Kvitsøy, Norway. This is an overtopping device i.e. its efficiency is directly proportional to the overtopping flows into the three reservoirs the device has one on top of each other. The overtopping flow rates have been measured separately for each one of them, together with incoming waves during physical model tests at Aalborg University. The influence of the significant wave height H_s and of the wave length L on the captured overtopping water is also described. It has been found that the performance of the SSG pilot plant will be negatively affected by spreading and directionality of the incoming waves as direct consequence of reduction on the overtopping flow rates of 10% - 35% compared to 2D conditions.

KEY WORDS: Wave energy; overtopping; breakwater; directional wave spectrum.

INTRODUCTION

Different Wave Energy technologies are competing in the Renewable Energy market after the huge energy potential they can benefit from has been proved. Developers' efforts are lately concentrated on demonstrating the reliability of the devices and on lowering the price per kW of produced power.

The SSG is a wave energy converter of the overtopping type. It has a number of reservoirs one on the top of each other specially designed to optimize the storage of potential energy of incoming waves from a specific wave spectrum. Efficiency is then directly proportional to the overtopping water temporarily stored in the reservoirs. The SSG pilot plant is a 10 m wide (capturing width) structure with three reservoirs one on the top of each other and installed capacity of 190 kW. The water temporarily stored in the reservoirs on its natural way back to the sea passes through turbines spinning them up and generating electricity. The pilot project at the island of Kvitsøy in Norway has been partially funded by the European Union FP6 and has the purpose of demonstrating the functioning of one full scale module of the SSG wave energy converter, including turbines and generators in 19 kW/m wave climate (Margheritini et al. 2008). In this case the reliability issue has been initially solved by realizing an "on shore" device where loads on the structure (Vicinanza et al. 2006) are considerably smaller than offshore, while the cost per kW compares prices of electricity for remote areas supplied by diesel generators. Nevertheless, when going

from offshore to shore the bathymetry can influence the overtopping flow rates i.e. the overall efficiency of the converter. Another promising application of the SSG concept is on breakwaters; but while the design of such structures is made to minimize overtopping and run up, the SSG design focuses on a combination of maximization of both these events. The purpose of the paper is to investigate the influence of 3D waves, irregular bathymetry and spreading on the overtopping flow rates for the 3 reservoirs of the SSG pilot plant at Kvitsøy location. The effect of H_s and L has also been investigated. The research has been done by mean of physical model tests in the deep wave tank of the hydraulic and coastal engineering laboratories at Aalborg University AAU equipped with 3D wave generator.

BACKGROUND OF THE STUDY

The overall efficiency of the device is the ratio between power output and the available wave power, given by the formula:

$$P_{wave} = \frac{\rho g^2}{64\pi} H_s^2 T_E \quad (1)$$

Where $\rho=1020 \text{ kg/m}^3$, $g = 9.82 \text{ m/s}^2$ and T_E is the energy period = $m-1/m0$, where m_n is the n -th moment of the wave spectrum defined as:

$$m_n = \int_0^\infty f^n \Phi(f) df \quad (2)$$

Φ , is the frequency spectrum. It is possible to consider the efficiency of the SSG overtopping device as a combination of partial efficiencies for every one of which it is necessary an optimization of parameters. The hydraulic efficiency is defined as:

$$\eta_{hy} = \frac{P_{crest}}{P_{wave}} \quad (3)$$

Where:

$$P_{crest} = \sum_{j=1}^3 q_{ov,j} R_{c,j} \rho G \quad (4)$$

$q_{ov,j}$ is the total overtopping flow rate for the j-reservoir and $R_{c,j}$ is the crest level of the respective reservoir (figure 1).

The overall efficiency of the device is then the combination of the hydraulic efficiency, storage efficiency (dependent on the reservoirs' volumes), turbines and grid connection efficiency. The design of the front of the SSG deals with the optimization of hydraulic performance.

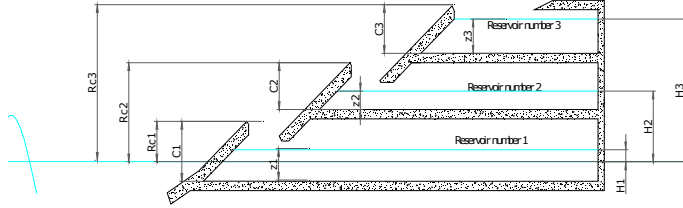


Figure 1. Definition sketch.

An expression for prediction of vertical distribution of overtopping has been suggested by Kofoed (2002) in the form:

$$Q' = \frac{dq/dz}{\lambda_{dr} \sqrt{gH_s}} = Ae^{\frac{Bz}{H_s} + C \frac{R_{c,1}}{H_s}} \quad (5)$$

Where Q' is the dimensionless of the overtopping discharge with respect to the vertical distance z and $R_{c,1}$ is the crest freeboard of the lowest reservoir. λ_{dr} is a coefficient describing the dependency of the draught and coefficients A , B and C need to be fitted to experimental data for the specific case. The eq.(5) is for long crested waves and horizontal bottom (2D model).

For the SSG pilot plant a number of 3 reservoirs has been chosen as adding extra reservoirs would only increase the hydraulic efficiency of 2 points percentage) (Kofoed 2006). 2D physical model tests have been carried out in order to optimize the geometry of the SSG pilot device (Kofoed 2005a). More than 30 geometries were tested under 2D irregular waves changing angles of the fronts, distances of the fronts, length of the fronts and crest levels. The analysis of overtopping flow rates in the 3 reservoirs from the best performing geometries lead to a set of coefficients A , B and $C = 0.197$, -1.753 and -0.408 respectively. As a result the final geometry has been defined with $R_{c,1,2,3} = 1.5$ m, 3m and 5m above SWL, angles of front = 35° and frontal front extended 5 meters under water level. An hydraulic efficiency of 50% has been estimated. 2D tests as such did not take into consideration the effect of bathymetry, directional wave spectrum and spreading, all phenomena that can influence the overtopping flow rates in the reservoirs.

EXPERIMENTAL SETUP

The model of the SSG used in laboratory was built at 1:60 scale and it was fixed rigidly on a 3D concrete model of the cliff located in the middle of the basin at 5 m from the paddles. The cliff is the best reproduction of the scanned bathymetry of the pilot plant location. The cliff has a very steep angle leading quickly to the sea bottom at -30 m CD. The pilot plant is more sheltered from waves coming from the left side as the cliff emerges from water (figure 2). The geometry of the model was realized according to the optimizations done by Kofoed, (2005a). The rear part of model was modified and equipped with four slopes leading to different small tank containers: one for each reservoir plus one for the overtopping over the whole structure. In this way infinite reservoir capacity was simulated. The captured overtopping water was temporally stored and then pumped out again in the basin by small pumps of known performance; the pumps were automatically activated when the water inside each container reached a pre-

established level (figure 3). By the total utilization of the pumps and the records of water levels inside the rear tanks, the overtopping volumes and flow rates have been derived for the single reservoirs.

The measuring equipment included:

- 4 wave gauges installed to measure time series of water levels in the reservoirs tanks.
- 7 resistive wave probes on a pentangle array placed on the plateau in front of the model, enabling the collection of data for 3D wave analysis.

Tested sea states

Tested wave conditions refer to operating conditions of the SSG pilot plant at Kvitsøy (Kofoed and Guinot, 2005b). The wave generation is controlled by the software AWASYSS, developed by laboratory research staff (<http://hydrosoc.civil.aah.dk/AwaSys/>). Generation of waves aimed to reproduce the following four offshore wave conditions: $H_s = 0.077$ m and $T_p = 1.37$ s; $H_s = 0.038$ m and $T_p = 1.02$ s; $H_s = 0.057$ m and $T_p = 1.20$ s; $H_s = 0.098$ m and $T_p = 1.51$ s; with constant water depth of 0.51 m. Tests have been carried out generating waves with head on attack angle ($D = 0$) and with an attack angle varying between -15° and 15° for each of the wave condition; no spreading condition was added to wave directions. Further, 9 spreading conditions were tested for each wave condition; these have been run with head on attack angle. A narrower directional spectrum corresponds to higher input spreading parameters ($S = 1000 \approx 2D \approx$ no spreading) as the directional spreading function adopted is expressed by a cosine power form.

2D conditions were also simulated in order to separate the effect of the 3D-ness of the structure from the effect of 3D wave spectrum. Each test comprised approximately 1500 waves.

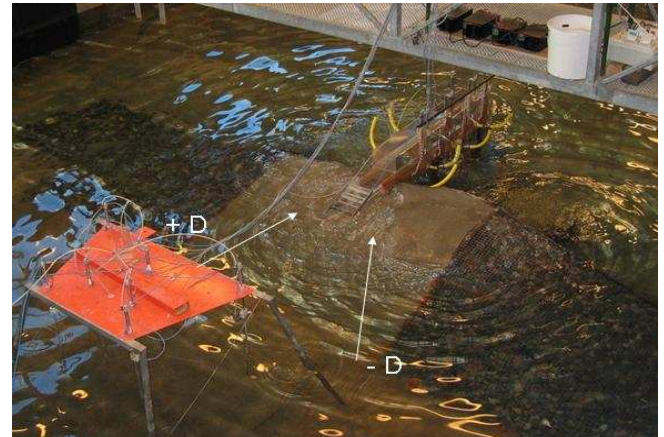


Figure 2. Tests setup. In evidence generated the wave directions.

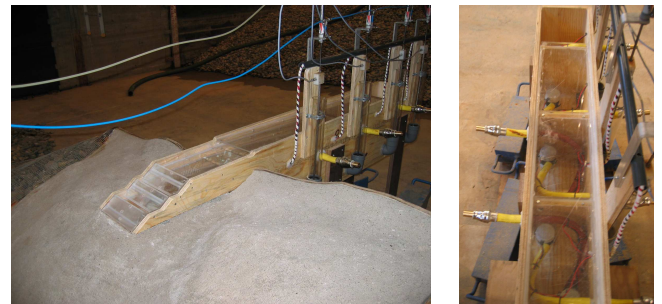


Figure 3. Details of the model in scale 1:60: on the left a top view of the rear tank containers equipped with pumps.

TEST RESULTS

Tests were carried out simulating spreading and different attack angles separated for each wave condition.

Dependency on the wave conditions

In figure 4 flow rates of the tests for the 3 reservoirs (q_1 , q_2 and q_3) are plotted for different spreading conditions. The results appear grouped in the graphics depending on the wave height (increasing with H_s). While little difference can be noticed comparing the 2D and the different spreading conditions for the same H_s in reservoir one and two, the difference between tests with low spreading ($\approx 2D$ conditions) and high spreading are relevant in reservoir three for higher H_s ; in this case higher spreading is limiting the amount of overtopping. In average an overall decrease by 10% of overtopping for the lower reservoirs and by 35% for the third reservoir is noticeable for situation with high spreading ($S < 100$) compared to situations without or with low spreading.

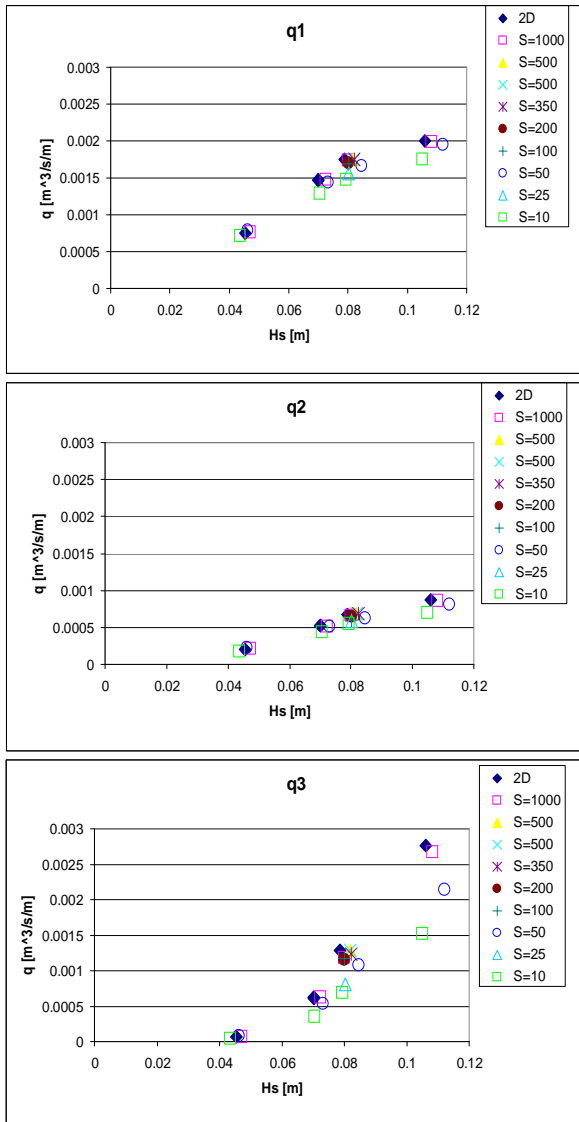


Figure 4. Dependency of the flow rates for the 1st, 2nd, and 3rd reservoir on H_s for different S and $D=0$. Scale model results.

In figure 5 the flow rates for the three reservoirs are plotted for different attack angles ($D = 0 =$ head on attack). Again little difference can be noticed in reservoir 1 and 2 when increasing D for the same H_s , while in reservoir number three the flow rates (q_3) are very influence by the directionality (attack angle and directional spreading): for waves higher then 0.08 m directionality of incidents waves decreases the overtopping. When increasing D we can see the same reduction on overtopping rates that occurred when increasing S .

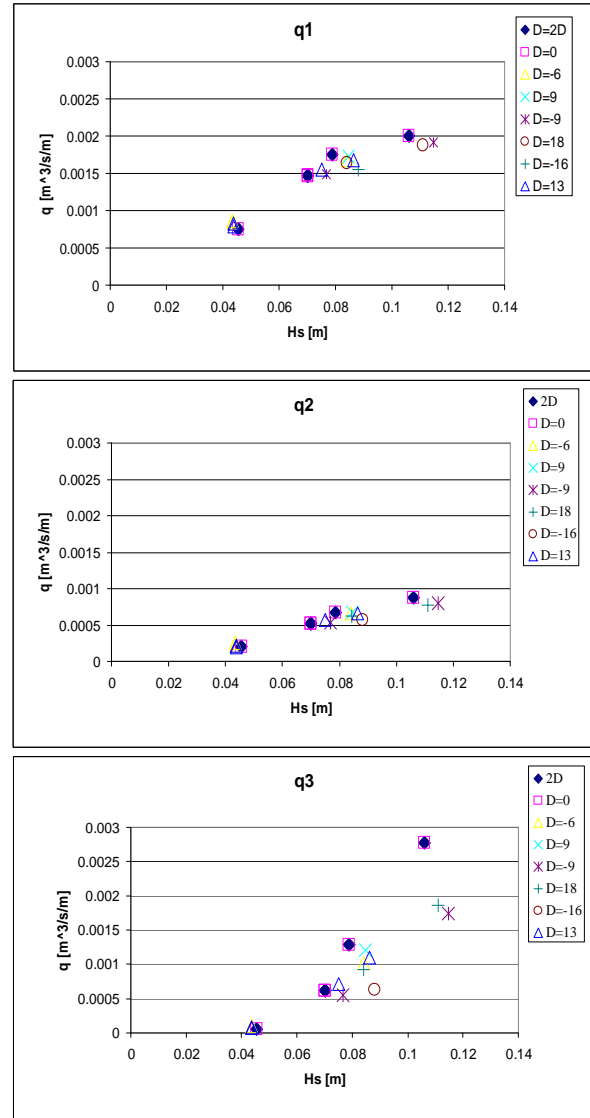


Figure 5. Dependency of the flow rates for the 1st, 2nd, and 3rd reservoir on H_s for different measured directions (attack angles in degree), no spreading. Scale model results.

The different trend that characterizes the dependency of the flow rates on H_s between reservoir one or two and reservoir three is due to the fact that the lowest ones have a roof while the highest one does not have any geometrical obstruction to the incoming flow. In other words it can be said that while the water to access the two lowest reservoirs has to enter in an opening, for the third reservoir the water needs to overtop a crest.

In general, the flow rates are higher in the third reservoir then in the lowest ones for bigger waves, according to expectations.

ANALYSIS OF RESULTS

Comparison with 2D test results

There is reasonable accordance when comparing the measured flow rates in the present set of tests in 2D conditions and in the 2D set of tests of Kofoed (2005a), figure 6. Nevertheless, it is possible to notice that there is better accordance to calculated results (integration of eq. 5) than to the measured results. At that time it was found that the formula was underestimating the flow rates for reservoir number 1 and number 3. In this case the better fitting of the measured results to the calculated data could be explained by the occurrence of a scale effect as the model used here is at scale 1:60 instead of 1:25 as in the compared tests and so boundary effects are more relevant. Indeed, apart from the scale and the presence of bathymetry, the sample of results compared here was produced for the same conditions (waves and geometry).

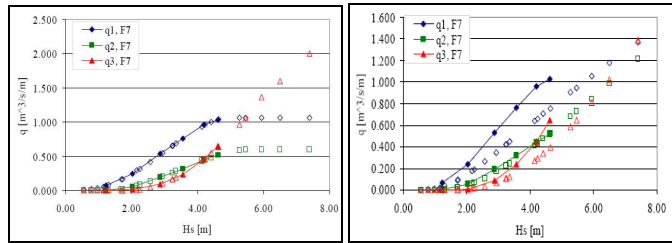


Figure 6. Model test results from Kofoed (2005a) for the same geometry of the present set of tests with inter and extrapolated data (open marks left) and with calculated data (open marks right).

Dependency on the wave length

By plotting the normalized overtopping flow rates against the R_C/L_{P0} (L_{P0} = offshore wave length referring to peak period T_p) for the different spreading conditions for reservoir 1 it can be noticed that before reaching a constant value around 0.02, the overtopping flow increases when decreasing L_{P0} , figure 7. For reservoir number 2 the constant value of 0.0075 is reached immediately, as shown in the same figure.

A completely different trend is found for flow rates in reservoir number 3: when the ratio R_C/L_{P0} increases the captured overtopping water decreases linearly for all the different spreading conditions (figure 8). This can be explained considering that the higher reservoir needs longer, bigger waves to be overtopped. By comparing the flow rates in the case with high spreading ($S=10$, dashed trend line) to the case with no spreading (2D, light continuous trend line) it is possible to estimate the losses of captured water in the higher reservoir.

The same behaviour can be found for the different reservoirs when plotting the normalized overtopping flow rates against R_C/L_{P0} for different attack angles of incoming waves: a longer wave “pumps” less water in first reservoir (figure 9) while increases the overtopping in the third reservoir (figure 10). This can be explained considering that steepest waves have a higher frequency and for the same time window more waves occur with shorter periods i.e. more water enters the first reservoir, but the height may be not enough to reach the higher reservoir. By comparison between the trend lines for the flow rates in the third reservoir for different directions, it seems obvious that the frontal attack ($D = 0$) brings more overtopping water than the cases when waves approach the structure with a certain angle. This is no longer evident when R_C/L_{P0} increases.

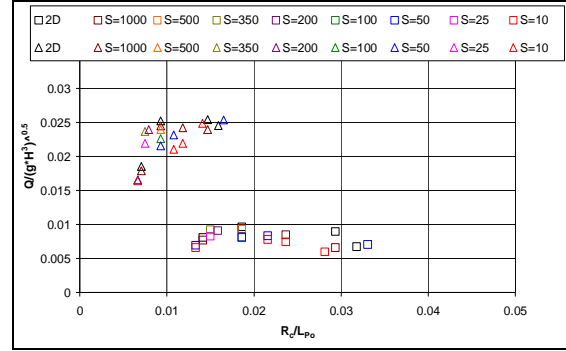


Figure 7. Dependency of the flow rates to reservoir no. 1 (triangles) and 2 (squares) on R_C/L_{P0} for different S.

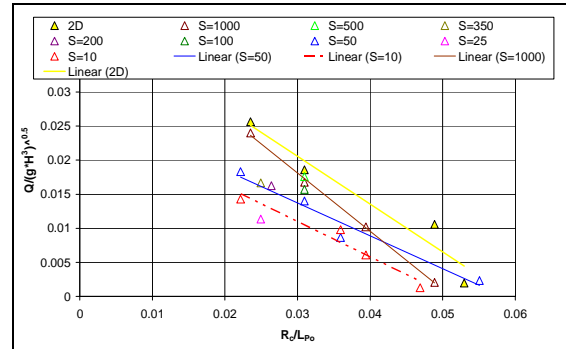


Figure 8. Dependency of the flow rates to reservoir no. 3 on R_C/L_{P0} for different S.

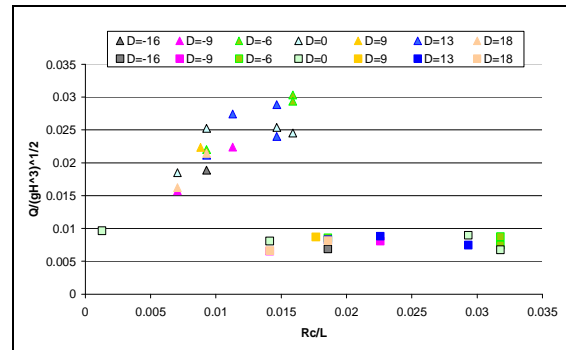


Figure 9. Dependency of the flow rates for reservoir no. 1 (triangles) and 2 (squares) on R_C/L_{P0} for different D.

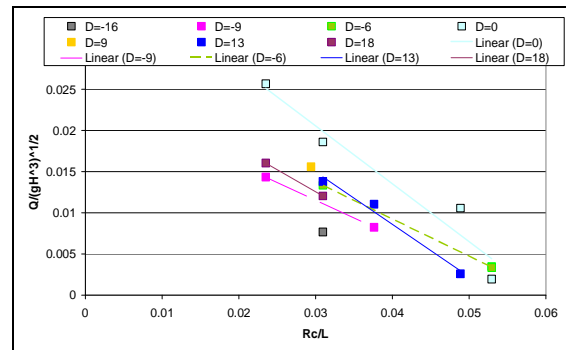


Figure 10. Dependency of the flow rates to reservoir no. 3 on R_C/L_{P0} for different D.

INFLUENCE OF 3D CONDITIONS

From the results presented in the previous section it is already possible to distinguish the effect of directional spectrum and spreading as reduction of overtopping water in the third reservoir (figures 8 and 10). It is also clear that the maximum overtopping in the different reservoirs occurs for different wave conditions. At the same time maximization of overtopping and optimization of the hydraulic efficiency are not the same thing as the last one aims to store bigger volumes selectively in the higher reservoirs.

In Figure 11 the calculated efficiency of laboratory tests with and without spreading is plotted against the efficiency with spreading divided by the efficiency without spreading (2D) for different wave conditions. W2, 3, 4 and 5 refer to the different tested wave conditions: W2: $H_s = 0.038$ m; $T_p = 1.02$ s. W3: $H_s = 0.057$ m and $T_p = 1.20$ s. W4: $H_s = 0.077$ m and $T_p = 1.37$ s. W5: $H_s = 0.098$ m and $T_p = 1.51$ s

In black the overall trend of the results depending on spreading. A local effect regards the wave condition number 2 (W2) and it could be imputable to the different interaction of the specific short period of the waves with the bathymetry.

In Figure 12 the calculated efficiency of laboratory tests with and without directionality is plotted against the efficiency with directionality divided by the efficiency without directionality (2D) for different wave conditions. Again the W2 condition behaves weirdly when adding attack angle $\approx \pm 9^\circ$. What all the tests present is an asymmetry of the graphic. This is in line with the differences in the bathymetry at the location objective of this study: when waves approach the structure with +D attack angles they do not meet the same small mound then they do with -D attack angles (figure 2), but a favorable slope. In this way waves coming from the right side of the dive face smaller dissipation of energy and reach the reservoirs easily.

It is assumed that the efficiency will not go to zero while increasing the attack angle of incoming waves from 0 to $\pm 90^\circ$. It is instead foreseen that the efficiency will stabilize around a certain value, also due to local effects caused by the wave-bathymetry interaction. The black line tries to represent this trend.

It is clear that directionality and spreading act on the same way on the overtopping for the three reservoirs of SSG pilot plant resulting in an overall reduction of the stored water up to 40%. This is specifically a problem for the SSG pilot plant as the device has a low width to depth ratio; in other words, because of the narrowness of the capture width, the lateral walls are an obstacle to the storage of overtopping water from incoming waves with an attack angle $\neq 0$. Because for overtopping of breakwaters an attack angle $-20 \leq D \leq 20$ is not considered to have significant effects on the overtopping flow rates (Wave Overtopping of Sea Defences and Related Structures: Assessment Manual 2007), it is reasonable to think that implementing more modules of the SSG device close to the others forming a line along a section of the coast or on a breakwater, this effect would be reduced. The phenomena that appear to have relevance when passing from 2D to 3D conditions are listed in table 1 with the evaluation of reduction of hydraulic efficiency from 50% realized in 2D conditions by Kofoed (2005a) for the specific case of the SSG pilot plant in the island of Kvitsøy.

Table 1. Reduction of the hydraulic efficiency from 2D to 3D conditions for the SSG pilot.

Reason of reduction of the η_{hy}	Average η_{hy}
- (2D conditions)	50%
Bathymetry	40%
Wave directionality	32%
Wave spreading	35%
Bathymetry+wave direction+wave spreading	$\approx 25\%$

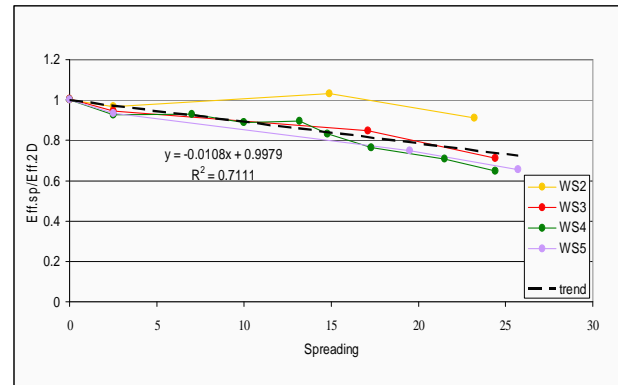


Figure 11. Influence of spreading on the hydraulic efficiency.

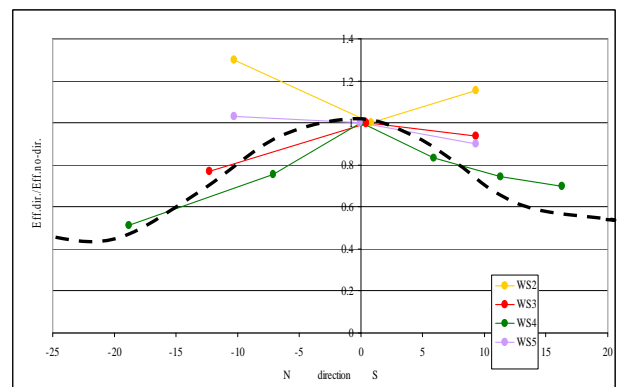


Figure 12. Influence of attack angle of incoming waves on the hydraulic efficiency.

CONCLUSIONS

By mean of 3D physical model tests in scale 1:60 to the SSG pilot plant in Kvitsøy it has been found that for bigger wave heights (and longer periods) the overtopping is higher in the third reservoir instead then in the lower ones; this is because the roof or the gaps between reservoirs one and two or two and three are setting an upper limit to the overtopping rates in reservoir one and two.

In general, to higher waves corresponds a higher volume of storage water in each of the three reservoirs.

It has also been found the effect of bathymetry: because of a non-symmetric, non-strait bottom, the overtopping flow rates are different for same $|D|$ but different directions.

By mean of 3D physical model tests and comparison with previous 2D set of tests with the same model geometry and wave conditions but different scale and no reproduction of local bathymetry, the influence of boundary conditions, wave directionality and wave spreading on the hydraulic efficiency of the SSG pilot plant has been found.

It is clear that the phenomena listed above act reducing the amount of overtopping water in the reservoirs and then the hydraulic efficiency of 50% in average. This reduction is strait forward the reduction on energy capture. The main limitation of the structure are related to its low width to depth ratio, as incoming waves with attack angles different from head on will be reflected by the side walls of the device and not enter the reservoirs. This explains while, even with as small attack angle as ones tested in the present discussion, a considerable reduction of water storage occurs.

REFERENCES

- Kofoed J. P. (2002): "Wave Overtopping of Marine Structures – Utilization of Wave Energy". Ph. D. Thesis, defended January 17, 2003 at Aalborg University. Hydraulics & Coastal Engineering Laboratory, Department of Civil Engineering, Aalborg University.
- Kofoed, J. P. (2005a): "Model testing of the wave energy converter Seawave Slot-Cone Generator", Hydraulics and Coastal Engineering No. 18, ISSN: 1603-9874, Dept. of Civil Eng., Aalborg University.
- Kofoed, J. P. and Guinot, F. (2005b): "Study of Wave Conditions at Kvitsøy Prototype Location of Seawave Slot-Cone Generator". Hydraulics and Coastal Engineering No. 25, ISSN: 1603-9874, Dept. of Civil Eng., Aalborg University, June, 2005.
- Kofoed, J. P. (2006): "Vertical Distribution of Wave Overtopping for Design of Multi Level Overtopping Based Wave Energy Converters", 30th International Conference on Coastal Engineering, ICCE San Diego.
- Margheritini, L., Vicinanza D., Frigaard, P. (2008): "SSG wave energy converter: design, reliability and hydraulic performance of an innovative overtopping device", submitted to *Journal of Renewable Energy, Elsevier*.
- Vicinanza, D., Kofoed, J. P. and Frigaard P. (2006), " Wave loadings on Seawave Slot-cone Generator (SSG) at Kvitsøy island (Stavanger, Norway)", Hydraulics and Coastal Engineering No. 35, ISSN: 1603-9874, Dep. Of Civil Eng., Aalborg University.
- Wave Overtopping of Sea Defences and Related Structures: Assessment Manual (2007), EurOtop.